

THE 4TH INTERNATIONAL CONFERENCE ON ALUMINUM ALLOYS

FLOW CHARACTERIZATION OF CAST Al-2Li

S. S. Menon and H. J. Rack
Materials Science and Engineering Program
Department of Mechanical Engineering
Clemson University
Clemson, SC 29631-0921, USA

Abstract

The constitutive behavior of cast Al-2 wt% Li has been characterized in the temperature range 573-823 K between strain rates 5×10^{-4} to 1 s^{-1} . These results, together with Dynamic Materials Modeling (DMM) were utilized to establish strain rate-strain-temperature processing maps. Stable regions, defined on the basis of two mechanistic stability criteria, $0 < m < 1$ and $\delta \log(m)/\delta \log(\dot{\epsilon}) < 0$ and two thermodynamic criteria, $s > 1$ and $\delta \log(s)/\delta \log(\dot{\epsilon}) < 0$, were found to be associated with dynamic recovery at low temperatures and dynamic recrystallization at higher temperatures. Unstable flow was observed at both low temperatures (573-623 K)/high strain rates (10^{-1} - 1 s^{-1}) and at high temperatures (773-823 K) / low strain rates (10^{-3} - $5 \times 10^{-4} \text{ s}^{-1}$). These instabilities were associated, respectively, with macroscopic shear band formation and dynamic grain growth.

Introduction

Enhanced performance through vehicle weight reduction is one of the primary driving forces behind the development of new aerospace materials. This reduction can be achieved by decreasing density or increasing strength and/or modulus, i.e., by increasing the materials specific stiffness and strength. Historically the specific properties of conventional aluminum alloys e.g. 2XXX and 7XXX, have been increased by increasing absolute strength, little benefit being gained in modulus or density. However Al-Li alloys offer the potential of decreasing density and increasing stiffness while maintaining adequate strength.

Although Al-Li alloys have been examined for many years, their low ductility and low short transverse fracture toughness continues to limit their applicability (1,2). These reduced properties have been attributed to a variety of factors including intense shear band deformation, segregation to grain boundaries arising from grain boundary precipitation and the formation of precipitate free zones (PFZs) (3,4). Unquestionably the ductility and fracture behavior of Al-Li should be, and has been shown to be, dependent on the alloy's prior thermo-mechanical history (5). For example, fracture toughness depends upon the alloy's grain orientation, whereas ductility is greatly influenced by the grain size. Unfortunately, few detailed examinations of the influence of processing variables, i.e., deformation strain, strain rate and

temperature, on the microstructure developed during ingot breakdown have been reported. This knowledge base is essential if the full potential of Al-Li alloys is to be realized. Manufacturing process control parameter selection also requires careful attention if desired properties are to be attained. This necessitates a process control strategy that takes into account the relationship between the pre and post-deformed microstructures and the processing conditions. Previous attempts at designing such process controls were based on either a knowledge of atomic processes that define selected deformation mechanisms (6) or mechanistic models for defect nucleation (7), applicable primarily to only a few simple alloy systems. A more recent approach, Dynamic Material Modeling (DMM), utilizes experimentally derived constitutive relationships, combining the principles of continuum mechanics with irreversible thermodynamics, to establish "stable" flow regimes for optimal processing (8). In this system certain elements are considered as stores and others, sources of energy, while the workpiece is considered to be the energy dissipator. The intrinsic ability of the material to dissipate power is then the most important criterion to be used in optimizing process control. For stable material flow behavior, the rate of energy input into the processing system cannot exceed the amount which the material system can dissipate while avoiding fracture and/or plastic instability. Four criteria must be met for stable flow (8):

$$0 < m < 1 \quad (1)$$

$$\left[\frac{\partial m}{\partial(\log \dot{\epsilon})} \right]_{T,e} < 0 \quad (2)$$

$$s > 1 \quad (3)$$

$$\left[\frac{\partial s}{\partial(\log \dot{\epsilon})} \right]_{T,e} < 0 \quad (4)$$

where m , is the strain rate sensitivity parameter given by

$$m = \left[\frac{\partial \ln \bar{\sigma}}{\partial \ln \dot{\epsilon}} \right]_{T,e} \quad (5)$$

and s , the entropy factor given by

$$s = \left(\frac{-1}{T} \right) \frac{\partial \ln \bar{\sigma}}{\partial \left(\frac{1}{T} \right)} \quad (6)$$

Several investigators (9-12) have validated these models for advanced materials where dynamic

recrystallization, dynamic recovery and dynamic spheroidization have been found to be associated with stable flow regions, unstable regions being associated with flow localization, wedge cracking, kinking and dynamic grain growth. This study has considered the applicability of DMM to the thermo-mechanical behavior of cast Al-2 wt% Li, correlating the microstructural changes observed during deformation at elevated temperatures with selected control parameters, i.e., strain, strain rate and temperature.

Experimental Procedure

The cast Al-2 wt% Li alloy was supplied by Westinghouse Savannah River Company, Aiken, South Carolina, as 300 mm dia \times 62.5 mm thick slab, chemical analysis of the as-received material, Table I, being performed by ALCAN International, Kingston, Ontario, Canada. Based on CDTA results (13) the cast alloy was homogenized, at 823 K for 24 hours, the grain structure, after homogenization, being equiaxed with a mean grain size of 3.12 μm .

In order to characterize the high temperature, high strain flow behavior of the alloy, isothermal compression experiments were performed on a MTS 880 system utilizing an ATS recirculating air furnace. Grooved cylindrical compression samples ($L=17.1$ mm, $D=11.5$ mm, $L/D=1.5$) were machined from the cast plates, the concentric grooves assisting in the retention and re-distribution of the high temperature graphite lubricant during deformation. All test specimens were heated to the deformation temperature at a constant rate of 5 K/min, soaked at the test temperature for 15 minutes prior to testing, tests being conducted at temperatures between 573 and 823 K. Compression testing to a true strain of 0.69 at five different constant true strain rates, 5×10^{-4} , 10^{-3} , 10^{-2} , 10^{-1} , 1 s $^{-1}$, were performed with the samples being quenched in cold water within 9 seconds after completion of the compression test.

Optical microscopy was then used to establish the microstructural basis for the observed "stable/unstable" flow regions. The specimens were initially prepared on SiC paper (120, 240, 320, 400, 600, 1000, 2400 grit), followed by diamond spray polishing with silk cloth (9 μm , 6 μm , and 3 μm) and final preparation using a colloidal silica solution on microcloth. This was followed by anodizing in a solution of 7 ml HBF $_4$, 5 g Boric acid and 93 ml of distilled water, at 25-30 V, 25 C for 1 minute with observation under crossed polarizers.

Results and Discussion

At low temperatures and high strain rates, the true stress-true strain behavior of cast Al-2 % Li alloy, after correction for friction and adiabatic heating, exhibited continuous strain hardening, Figure 1. Decreasing strain rate and/or increasing temperature resulted in a gradual reduction in the degree of strain hardening, steady state flow being observed at high strains, Figure 2.

The strain rate sensitivity calculated at two different strains, viz. 0.2 and 0.5, was found to be a function of strain rate and temperature, Figure 3, the maximum value (0.6) being observed at 750 K and a strain rate of 5×10^{-4} s $^{-1}$. Stable/unstable regions for cast Al-2%Li defined on the basis of two mechanistic stability criteria, $0 < m < 1$ and $\delta m / \delta \log \dot{\epsilon} < 0$, Figure 3, shows a single instability at low temperatures/high strain rates, the size of the unstable region being independent of strain. Similarly, the entropy factor, s , as defined by Equation 6, was a function

Table I. Results of Chemical Analysis

Composition	pct by weight					
	Li	Na	K	Fe	Si	Cu
Cast Al-2% Li	1.94	.0005	.0006	.001	<.005	<.002

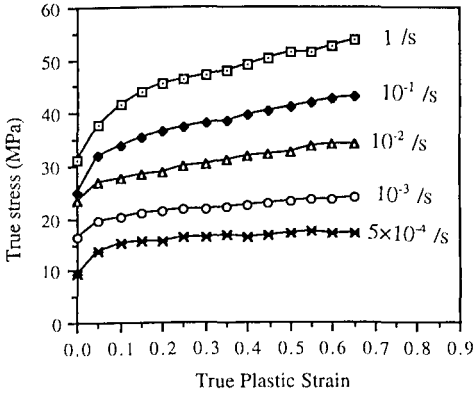


Figure 1. True stress-true strain curves for cast Al-2 wt% Li at 573 K

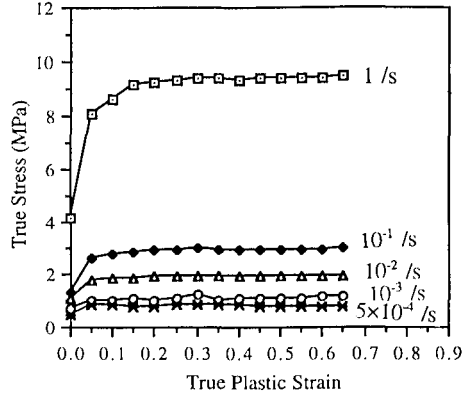


Figure 2. True stress-true strain curves for cast Al-2 wt% Li at 823 K

of strain rate and temperature, Figure 4. This factor increased with increase in temperature, the maximum value (7.4) being attained at 823 K and a strain rate of $10^{-1.5} \text{ s}^{-1}$. In addition,

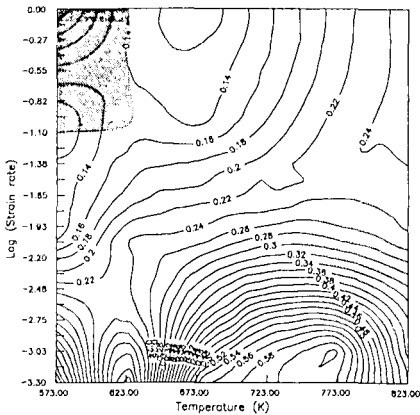


Figure 3. Strain rate sensitivity, m , contour for cast Al-2 wt% Li ($\epsilon = 0.5$). Shaded area represents region of instability.

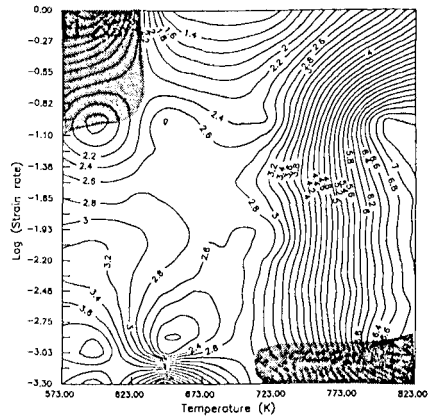


Figure 4. Entropy factor, s , contour map for cast Al-2 wt% Li ($\epsilon = 0.5$). Shaded areas represent regions of instability.

Figure 4 shows two regions of instability, based on the two thermodynamic stability criteria, $s > 1$ and $\delta s / \delta \log \dot{\epsilon} < 0$, one within the same low temperature/high strain rate region observed utilizing the mechanistic stability criteria, the other at higher temperatures/ lower strain rates. Again, the extent of both regions was not dependent on deformation strain.

The activation energies associated with elevated temperature flow was also determined by assuming that this behavior could be described by the power law relationship,

$$\dot{\epsilon} = A \cdot \exp\left(\frac{-Q}{RT}\right)$$

where R, is the universal gas constant and Q the activation energy. The activation energy can then be expressed as a function of m and s by,

$$\frac{-Q}{R} = \left[\frac{\partial \ln \sigma}{\partial (1/T)} \right] \left[\frac{\partial \ln \dot{\epsilon}}{\partial \ln \sigma} \right] \quad (8)$$

substituting equations (5) and (6) yields,

$$Q = \frac{sRT}{m} \quad (9)$$

Combining the four DMM stability criteria with the activation energy analysis shows that stable flow was observed over a wide temperature and strain rate range, Figure 5. Within this stable region the activation energy at low temperatures exhibited a broad minima, gradually increasing with increasing temperature. This variation suggests that at low temperatures the primary flow mechanism involves dislocation cell growth (recovery), that is the activation energy is associated with atomic motion across a cell boundary (14). With increasing temperature the activation energy is associated with 3-dimensional growth and approaches that of Li diffusion in Al-Li (15). Unstable flow was restricted to narrow regions either at low temperature/ high strain rates or high temperatures/low strain rates.

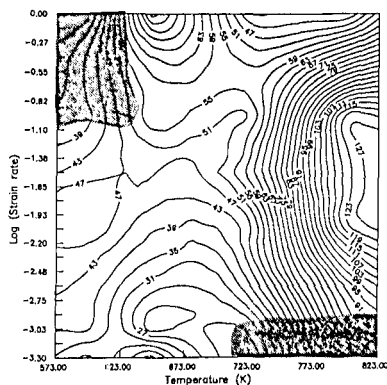


Figure 5. Activation energy(kJ/mole) contour map for cast Al-2 wt% Li ($\epsilon = 0.05$). Shaded areas represent the instability regions determined by considering all DMM stability criteria.

Metallographic observations, Figure 6, indicated that the instability observed at low temperatures (573 K - 623 K) and high strain rates ($10^{-1} - 1 \text{ s}^{-1}$) was associated with flow localization and the formation of macro shear bands. Specimens deformed within the instability regions observed at high temperature (773-823 K) and low strain rates ($10^{-3} - 5 \times 10^{-4} \text{ s}^{-1}$) revealed that these conditions was associated with dynamic grain growth, Figure 7(a). This conclusion was supported by comparing the microstructure of a deformed specimen with that of a specimen heated to 823 K and soaked for a time equivalent to the deformed sample. Figure 7(b) shows that the grain size of the latter was substantially smaller than that of the deformed sample, indicative of strain assisted grain growth.

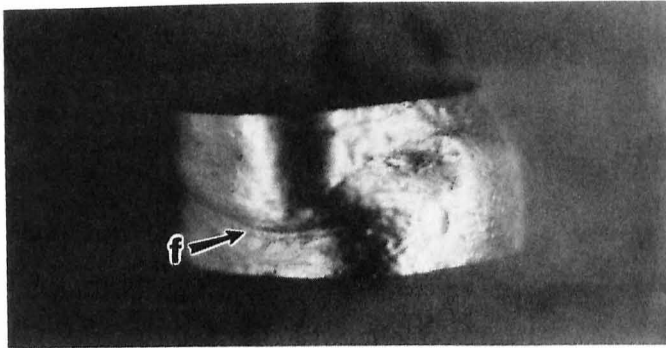


Figure 6. Flow localization (f) in cast Al- 2 wt% Li deformed at 573 K/1 s^{-1} .

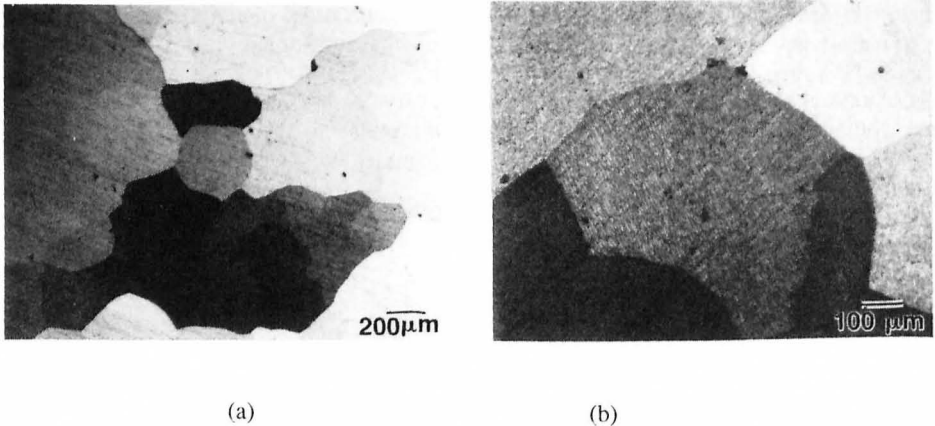


Figure 7. Optical micrograph showing (a) dynamic grain growth at 823 K/ $5 \times 10^{-4} \text{ s}^{-1}$ (b) undeformed specimen heated to 823 K and soaked for 15 min.

Finally, examination of samples deformed within the stable flow regions supported the prior activation energy analysis. At low temperatures (623 K-723 K) deformation was associated with dynamic recovery, Figure 8, this stable dissipative process gradually transitioning to dynamic recrystallization at higher temperatures (723 K- 773 K), Figure 9.

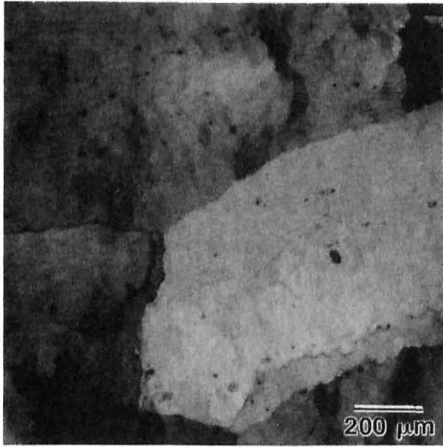


Figure 9. Dynamic recovery at 673 K and a strain rate of 10^{-2} s^{-1} .

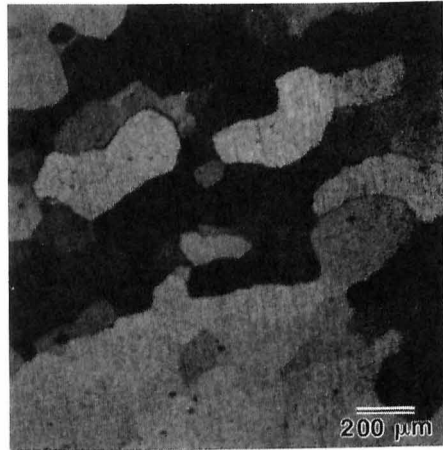


Figure 10. Dynamic recrystallization at 773 K and a strain rate of 10^{-3} s^{-1} .

Conclusions

At low temperatures and high strain rates the true stress-true strain behavior of cast Al-2 % Li alloy exhibited continuous strain hardening, decreasing strain rate and/or increasing temperature resulting in a gradual reduction in the degree of strain hardening, steady state being observed at high strains.

Dynamic Materials Modeling (DMM) can be utilized to summarize the flow behavior of cast and homogenized binary Al-Li alloys. Two regimes of instability were observed and related to macroscopic flow localization at low temperatures/high strain rates and dynamic grain growth at higher temperatures/lower strain rates. Stable flow regions were associated with dynamic recovery at low temperature and dynamic recrystallization at higher temperatures.

Acknowledgements

This project was sponsored by the Westinghouse Savannah River Company (WSRC), Aiken, South Carolina, Dr. Nataraj Iyer, acting as contract monitor. The authors wish to thank Dr. David Lloyd of ALCAN, Kingston, Ontario, Canada, for performing the chemical analysis of the Al-2% Li alloy and to Mr. Sarup Chopra of Alcoa, Alcoa Center, Pennsylvania, for his assistance in developing the metallographic procedures.

References

1. J. T. Staley, Light Metal Age, December 1990, 31.
2. D. B. Williams, Aluminum-Lithium Alloys, ed. T. H. Sanders, Jr. and E. A. Starke, Jr., (The Metallurgical Society of AIME, Warrendale, PA, 1980), 89.

3. P. J. Gregson, C. J. Peel and B. Evans, Aluminum Lithium Alloys III, C. Baker, P. J. Gregson, S. J. Harris and C. J. Peel, Institute of Metals, London, 1986, 222.
4. T. H. Sanders, Jr., Aluminum-Lithium Alloys, ed. T. H. Sanders, Jr., E. A. Starke, Jr., (The Metallurgical Society of AIME, Warrendale, PA, 1980), 63.
5. A. Gysler, R. Crooks and E. A. Starke, Jr., Aluminum-Lithium Alloys, ed. T. H. Sanders, Jr., E. A. Starke, Jr., (The Metallurgical Society of AIME, Warrendale, PA, 1980), 189.
6. H. J. Frost and M. F. Ashby, Deformation-Mechanism Maps, The Plasticity and Creep of Metals and Ceramics, (Pergamon Press, New York, 1982).
7. R. Raj, Metall. Trans. A, 12A, 1981, 1089.
8. H. L. Gegel, J. C. Malas, S. M. Doraivelu, J. M. Alexander and J. S. Gunasekera, Advanced Technology of Plasticity, K. Lange, ed. Springer-Verlag, Berlin, 1987, Vol. 2, pp. 1243-1250.
9. J. C. Malas, Ph. D. Dissertation, Ohio University, Athens, Ohio, (1991).
10. M. Long and H. J. Rack, Mater. Sci. and Engg., A170, 1993, 215.
11. S. Guillard, Ph.D Dissertation, Clemson University, Clemson, SC (1994).
12. N. Ravichandran and Y. V. R. K. Prasad, Metall. Trans., 22A, 1991, 2339.
13. S. S. Menon, M.S. Thesis, Clemson University, Clemson, SC, (1994).
14. M. Avrami, J. Chem. Phys, 7, 1939, 1103.
15. P. G. Partridge, International Materials Reviews, 35, No. 1, 1990, 37.